

GLOBAL GRADIENT ESTIMATION OF HYPERSPECTRAL IMAGES FOR REGISTRATION REFINEMENT IN MULTIMODAL MICROSPECTROSCOPY

Ch. Pomrehn^{1*}, A. Kolb², R. Herpers^{1,3,4}

¹Institute of Visual Computing, Bonn-Rhein-Sieg University of Applied Sciences, Germany

²Institute for Vision and Graphics, University of Siegen, Germany

³Faculty of Computer Science, University of New Brunswick, Canada

⁴Lassonde School of Engineering, York University, Canada

ABSTRACT

This contribution introduces a new methodology for the automated estimation of grayscale representations for hyperspectral images (HSI) in the context of multimodal vibrational microspectroscopic imagery. The purpose of the estimated image is to enable a refinement in intensity-based registration of already coarsely registered HSI. The proposed approach derives and fuses gradient information that are globally distributed in the spectral domain using image data from conventional brightfield microscopy (BFM) as a guidance and anchor image for indirect refinement of HSI registration. It is demonstrated that the global gradient image estimated by solving two different optimization problems, reliably improves device-based registration of HSI generated by Raman microspectroscopy (RMS) and infrared microspectroscopy (IRMS).

Index Terms— Hyperspectral Image, Registration Refinement, Multimodal Microspectroscopy, Correlative Microscopy

1. INTRODUCTION

The scientific term *correlative microscopy* generally comprises the usage of different microscopy techniques, combined in a common imaging approach. In recent years, an increasing trend in researching these multimodal imaging techniques has been observable. Its consistent development emphasizes the growing importance of multimodal concepts for image-based analysis. Among others, vibrational microspectroscopy (VMS) has proven to be a promising candidate for successfully combining spectral information in a multimodal imaging approach. Here, VMS unifies the complementary concepts of RMS and IRMS.

As imaging techniques, both methods enable material specific spectral information to be determined from re-emitted radiation after a point-wise excitation of the sample. The set of rastered individual measurements can be represented as a HSI. As the demand for multimodal approaches in VMS or comparable microscopic concepts increases so does the need for partially or fully automated analysis procedures. For image-based evaluation of multimodal approaches, automated and accurate registration of images from the different modalities is essential. Related to HSI, the task of image registration might become even more challenging, in comparison to other established imaging techniques, as the spatial information is distributed over multiple channels in the spectral domain. Thus, the generation of an image appropriate for registration often needs expert knowledge to select spectral bands that are representative of the components of the object under investigation, as presented in Fig. 1. Additionally, the different modalities often provide significant differences in spatial resolution, as in IRMS and RMS.

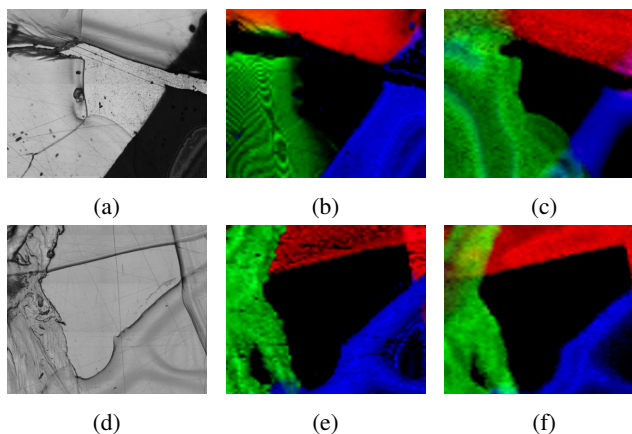


Fig. 1: Multimodal image data of two polymer samples providing three different components. BFM images (a) and (d), univariate visualization of RMS data (b) and (e) as well as IRMS data (c) and (f).

*This work was partly funded by the German Research Foundation (DFG) as part of the research training group GRK 1564 *Imaging New Modalities*. We further acknowledge the doctoral scholarships of the Department of Computer Science at the Hochschule Bonn-Rhein-Sieg University of Applied Sciences, as well as the contribution to this work by Daniel Klein.

Consequently, spatial information provided by one modality might be missing in the other due to different diffraction limitations of the imaging systems. For these reasons, a cross-modal matching of *interest points*, as often used for *landmark-based* image registration approaches, might become impractical. Consequently, it is more reasonable to prefer intensity-based approaches to ensure a successful automated registration of hyperspectral images in VMS. However, even intensity-based registration requires an appropriate representation of the local sample structure, ideally as a grayscale image.

The automated estimation of such a grayscale representation from out of a hyperspectral image structure, has not yet been extensively addressed in research related to VMS. Thus, the purpose of this contribution is to introduce a corresponding concept for estimating a global gradient image from HSI data. Thereby, we benefit from a grayscale image from conventional BFM, as used when parameterizing the individual spectroscopic measurements, illustrated in Fig. 1. In a first step, the BFM images serves as a guidance image to extract spatial information from the spectral domain of the HSI. In a second step, it serves as an anchor image for compensating slight misregistration to the generated HSI, which occur after measurements with device-based registration, as presented in Fig. 2. Using the same anchor image for intensity-based registration refinement in both considered modalities, should lead to appropriate registered HSI. First results demonstrate that the gradient image estimated by the proposed methodology, reliably enables intensity-based registration refinement for HSI data, showing different scales of misregistration.

To give detailed insights to the proposed concept, the remainder of this paper is organized as follows. In Section 2 a brief statement concerning the given problem is presented and a general approach for its solution is proposed. In Section 3, comparable approaches for estimating global gradient images from HSI, related to *correlative microscopy*, are presented from the literature. A detailed description of the developed methodology is given in Section 4.1. Experimental results of the proposed solution and registration refinement evaluation in Section 5, are followed by a discussion in Section 6 and a conclusion in Section 7.

2. PROBLEM STATEMENT

A basic prerequisite for processing hyperspectral image data in a multimodal approach of VMS is an appropriate accuracy in registration. In turn, an image representation is required that provides sufficient spatial features to enable a precise registration. For this purpose, an automated methodology is needed, extracting relevant features globally along the spectral domain and fuses it into a single grayscale image. Due to the different spatial resolution in RMS and IRMS and the complementary spectral information of both modalities, established feature extraction methods for landmark-based

registration, such as SIFT [1], SURF [2] or KAZE [3] features, as investigated in [4, 5, 6] for HSI in the context of remote sensing, might become challenging for cross-modal matching in VMS. The approach introduced in this contribution, is based on the assumption that the local structure of a sample, required for intensity-based registration, is globally derivable from the gradient information of the individual spectral channels.

We therefore make use of a BFM grayscale image, as it is needed to parameterize the optical measurements setup for HSI generation in VMS. The proposed methodology intends to use gradient information from the BFM image as a guidance for extracting gradient information globally from the HSI. Therefore, a sufficient spatial correlation of the already coarsely registered images is assumed. The proposed methodology is implemented in the context of a multiresolution analysis approach where in each decomposition level, the following optimization problem is considered.

Let $\mathbf{P} \in \mathbb{R}^{n \times m}$ be a grayscale image of the object under investigation and $\nabla \mathbf{P}$ its corresponding gradient magnitude representation determined by the a *Sobel* operator. Let $\mathbf{HS} \in \mathbb{R}^{n \times m \times \lambda}$ be a hyperspectral image and $\nabla \mathbf{HS}_i$ the gradient magnitude representation of its i -th channel in the spectral domain determined by the *Sobel* operator. The purpose of the introduced methodology is the data dependent generation of a global gradient image $\nabla \mathbf{G}$ derived from the hyperspectral gradient representations $\nabla \mathbf{HS}_i \forall i = 1, \dots, \lambda$ such that

$$|\nabla \mathbf{P} - \nabla \mathbf{G}| \rightarrow \min \quad (1)$$

It is assumed that the gradient image estimated by equation 1, is appropriate for intensity-based registration of $\nabla \mathbf{P}$ and $\nabla \mathbf{G}$. To enable registration refinement of the HSI across the different spectroscopic modalities, $\nabla \mathbf{P}$ serves as an anchor image and thus, indirectly ensures precise registration of the HSI from VMS.

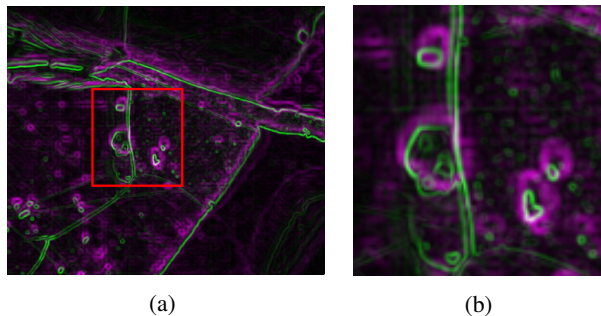


Fig. 2: Deviations in the registration accuracy achieved by device-based registration. Global sample representation in (a) and up-scaled region of interest (b) emphasizing the potential for registration refinement of BFM and VMS image data.

3. IMAGE ESTIMATION FOR INTENSITY-BASED REGISTRATION OF HSI

Over the last decade, multimodal approaches for *correlative microscopy* have become increasingly important. Accordingly, several solutions for estimating appropriate images are proposed in the literature, intending to enable an intensity-based registration of HSI. In [7], Kwak et al. combined IRMS and BFM for the automated histological analysis of prostate cancer in tissue samples. Here, images for intensity-based registration purposes were estimated, extracting characteristic parts of the tissue samples by binarization of the original HSI. A comparable approach is presented by Chang et al. in [8], where registration is conducted using a pre-segmented HSI derived by k-means clustering. In [9], Gowen et al. derive an appropriate image for registration of RMS and IRMS data by a binarization of the first principal components of HSI in each modality. In [10], Allouche et al. introduced a *template matching* related approach for registration and coupling image data from BFM, RMS and IRMS. The HSI representation $\widetilde{\mathbf{HS}}$, used for registration purposes, was determined by the sum of pixel intensities over the λ channels of the spectral domain

$$\widetilde{\mathbf{HS}} = \sum_{i=1}^{\lambda} \mathbf{HS}_i. \quad (2)$$

In [11], Penaranda et al. used a statistical-based image estimation for a refinement in a two-step registration approach. There, the image was the complement image of \mathbf{HS}_{std} , derived by the standard deviation of each spectral pixel signature,

$$\mathbf{HS}_{\text{std}} = \sqrt{\frac{1}{\lambda-1} (\widetilde{\mathbf{HS}} - \overline{\mathbf{HS}})^2}, \quad (3)$$

where $\overline{\mathbf{HS}}$ contains the mean value for each spectral pixel vector. In [12], Trukhan et al. lately made usage of the *extended multiplicative signal correction* model [13] to derive an intensity-based image that is directly related to the optical path length in a *Beer-Lambert's* absorbance process. The estimated image was found to be highly representative for the actual spatial structure of the sample.

To summarize, the methods presented in the literature are either based on binarization resp. classification of the pixel vectors or on basic arithmetical and statistical models. Physically motivated models are rare. To the best of the authors knowledge, taking into account an image from a further modality, for guidance and anchor purposes, is a new methodological approach in the context of *correlative microscopy*. The integration of additional and highly resolved spatial information into the image generation process and into the registration procedure, might lead to more tailored images and thus, to more accurate results for intensity-based registration.

4. PROPOSED PROBLEM SOLUTION

4.1. Problem Formulation

The problem introduced in Section 2 is considered as a linear optimization problem. With $\nabla \mathbf{P}$ and

$$\nabla \mathbf{G} = \sum_{i=1}^{\lambda} x_i \nabla \mathbf{HS}_i \quad (4)$$

the purpose is to find the vector $x \in \mathbb{R}^{\lambda}$ that minimizes the objective function in equation 1, in a non-negative least square sense by

$$\min_{x \geq 0} \|\nabla \mathbf{P} - \nabla \mathbf{G}\|_2^2. \quad (5)$$

The optimization task is implemented in the context of a multiresolution analysis approach, which solves the optimization problem on K different decomposition levels of a Gaussian pyramid. The concluding reconstruction for the gradient images $\nabla \mathbf{X}$ and $\nabla \mathbf{Y}$ is estimated from the results of $\nabla \mathbf{G}_k$ resp. $\nabla \mathbf{P}_k$, upscaled to the initial image dimension using bicubic interpolation, using the linear models

$$\nabla \mathbf{X} = \sum_{k=1}^K \alpha_k \nabla \mathbf{P}_k \quad (6)$$

as well as

$$\nabla \mathbf{Y} = \sum_{k=1}^K \beta_k \nabla \mathbf{G}_k. \quad (7)$$

The corresponding weighting vectors α and β , restricted to

$$\sum_{k=1}^K \alpha_k = 1 \quad \text{and} \quad \sum_{k=1}^K \beta_k = 1, \quad (8)$$

are either empirically selected based on the visual assessment of $\nabla \mathbf{G}_k$ resp. $\nabla \mathbf{P}_k$ or automated by solving a further optimization problem. Therefore, the weighting vectors α and β are estimated from the unfolded matrix representation of $\nabla \mathbf{G}_k$ resp. \mathbf{P}_k with $\widetilde{\nabla \mathbf{G}} \in \mathbb{R}^{NM \times K}$ and $\widetilde{\nabla \mathbf{P}} \in \mathbb{R}^{NM \times K}$, where N and M denote the pixel dimension of $\nabla \mathbf{G}_k$ and $\nabla \mathbf{P}_k$ respectively, by solving

$$\min_{\alpha, \beta \geq 0} \frac{1}{NM} \|\widetilde{\nabla \mathbf{P}} \alpha^T - \widetilde{\nabla \mathbf{G}} \beta^T\|_2^2. \quad (9)$$

From equations 9, a general formulation of the multimodal and intensity-based registration problem, considering an affine transformation Φ and the mean squared error (MSE) as similarity metric, is given by

$$\min_{\Phi} \frac{1}{NM} \|(\nabla \mathbf{X} - \Phi(\nabla \mathbf{Y}))\|_2^2. \quad (10)$$

4.2. Problem-based Optimization Implementation

The optimization problem introduced in equation 1 was treated as a *Non-Negative Partial Least Square* problem, solved by using the algorithms introduced by Lawson et al. in [14]. To estimate the reconstruction weights α and β , a problem-based minimizing setup was implemented, using the *Optimization Toolbox* provided by Matlab. Here, equation 9 was defined as objective function. The weighting vectors α and β , with 0 as lower and 1 as upper bounds, were defined considering the constraints in equation 8. The optimization problem was solved by applying *Dual Simplex* algorithm. The estimation of the affine transformation Φ was realized by using established registration algorithms of the *Image Processing Toolbox* provided by Matlab.

5. EXPERIMENTAL RESULTS

5.1. Hyperspectral Image Data

To evaluate the presented methodology, image data of two different polymer samples was used, with each sample consisting of three different components with individual spectral signature. RMS and IRMS images were acquired by applying a point-by-point mapping procedure of 4900 resp. 5625 measuring points. For RMS, a laser excitation wavelength of 785 nm was used. Spectral information of the first polymer sample covers a wavenumber range from 710 to 1790 cm^{-1} . For the second polymer sample, a wavenumber range from 150 to 1560 cm^{-1} was considered. For IRMS image data, absorbance spectra of the wavenumber range from 600 to 3230 cm^{-1} have been collected for the first polymer sample and from 600 to 3300 cm^{-1} for the second sample, respectively. All HSI have been preprocessed according to state-of-the-art procedures, including outlier removal, normalization, baseline correction and spectral smoothing. To create a more explicit initial misregistration, HSI data of the polymer sample presented in Fig. 1 (e) and (f), has been spatially cropped. Thus, the applicability of the presented approach with respect to larger spatial deviations is investigated as well. All images have been spatially scaled to a size of 350 \times 415 pixel.

5.2. Results of Proposed Solution

The estimation of global gradient images introduced in Section 4.1 was investigated using HSI data from BFM and VMS, as presented in Section 5.1. By solving the optimization problems defined by equation 5 and 9 in a fully automated procedure, ∇X and ∇Y have been generated according to equations 6 and 7. The results are presented in Fig. 3. The corresponding estimates of the weighting vectors α and β are given in Table 1. In addition, the proposed methodology has been investigated as a semi-automated approach. For this, the weighting vectors α and β were chosen based on visual assessment of the estimates for ∇G_k and ∇P_k .

Table 1: Estimates for weighting vectors α and β from equation 9. Letter indices denote considered modality IRMS (IR) or RMS (R). Numeric indices corresponds to the polymer sample used. Note that values smaller $1.0 e^{-3}$ are replaced by 0.00 due to the negligible contribution.

K	α_{IR^1}	β_{IR^1}	α_{R^1}	β_{R^1}	α_{IR^2}	β_{IR^2}	α_{R^2}	β_{R^2}
0	0.62	0.53	0.50	0.42	0.68	0.55	0.59	0.45
1	0.00	0.00	0.00	0.00	0.00	0.00	0.00	0.00
2	0.10	0.07	0.09	0.00	0.00	0.04	0.00	0.1
3	0.28	0.40	0.41	0.58	0.32	0.41	0.41	0.44

5.3. Registration Refinement Evaluation

According to the general concept of the introduced approach, it is clear that verifying its effectiveness for registration refinement requires a two-step evaluation procedure. In a first step, an intensity-based registration was applied to the estimates of anchor image ∇X and the global gradient image of the corresponding HSI ∇Y . In the case of a successful registration, the achieved improvement in accuracy was determined after applying the estimated affine transformation Φ to the original HSI data. In a second step, the improvement in accuracy of HSI registration refinement was evaluated. Therefore, a comparison of the original and the transformed HSI data was conducted. It has to be stated here that an intended comparison to the registration accuracy achieved by images computed from equation 2 and 3 was not possible, as the corresponding intensity-based registration refinement does not lead to satisfying results.

5.3.1. HSI and Anchor Image Registration

An interactive evaluation procedure was implemented to estimate the achieved registration accuracy. Thereby, *interest points* that were visually recognizable in the edge progressions of both images, were marked manually in a superimposed visualization of the anchor image and an univariate visualization of original HSI data. The euclidean distance between the marked position served as metric for registration accuracy. The procedure was conducted before and after applying the estimated affine transformation Φ from 9, to the original HSI data. Three identified *interest points* were manually selected in N=10 evaluation run. The estimated averaged euclidean distance for the selected points are presented in Table 2 for HSI of the first polymer sample and in Table 3 for HSI of the second polymer sample, respectively. Here, the numerical indices denotes the interest point that was considered, while the letter indices b and a indicates distance estimation before and after applying registration refinement. The indices of the considered modalities IRMS and RMS illustrates, whether the weighting vectors α and β have been determined automatically (A) by solving equation 9 or have been chosen manually (M) based on visual assessment of ∇P_k .

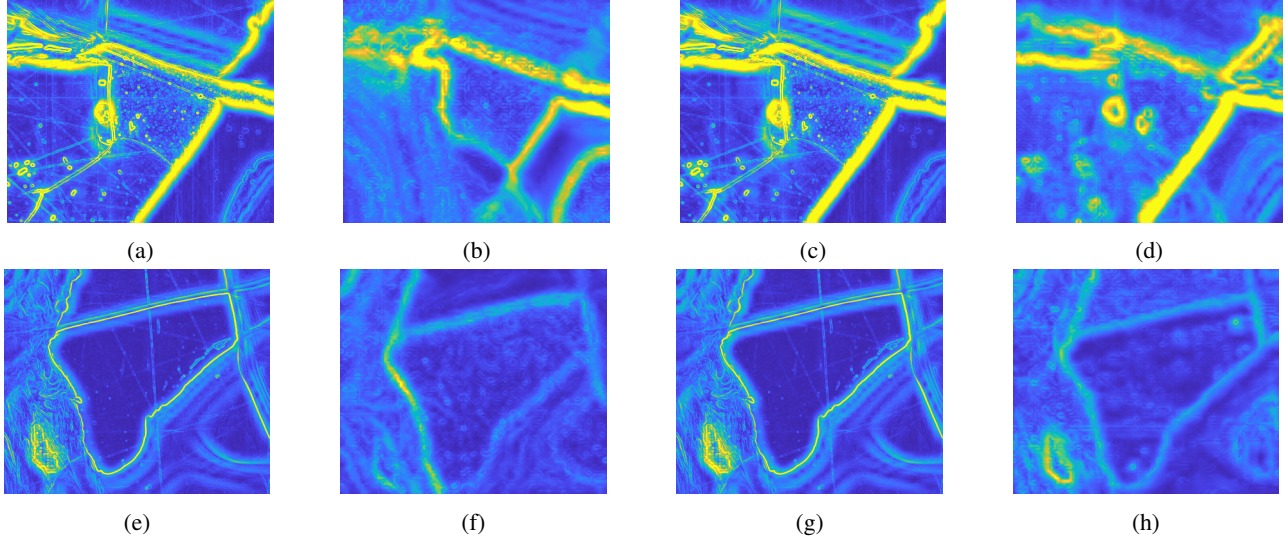


Fig. 3: Images derived from equation 6 and 7 for first polymer sample (a)-(d) and second polymer sample (e)-(h). ∇X for IRMS registration (a), estimated gradient image ∇Y from IRMS data (b), ∇X for RMS registration (c), estimated gradient image ∇Y from RMS data (d). ∇X for IRMS registration (e), estimated gradient image ∇Y from IRMS data (f), ∇X for RMS registration (g), estimated gradient image ∇Y from RMS data (h).

As the methodology intends a refinement in registration, smaller distances indicate greater accuracy. For the HSI data of both considered samples, a unique improvement in registration accuracy could be achieved by using the estimated global gradient image in intensity-based registration. The averaged distances in the last two columns confirm the visual assessment of registration result, as exemplary shown in Fig. 4. The improvement is observed for fully and semi-automated implementations.

5.3.2. HSI Registration Refinement

To evaluate the registration refinement with respect to the HSI data from VMS, a similar interactive evaluation procedure was conducted. Here, *interest points* were marked in superimposed images of gradient information from the corresponding univariate visualizations of the HSI. Evaluation was performed before and after applying the estimated affine transformation Φ from 9 to the original HSI data. As in 5.3, the euclidean distance serves as evaluation metric to verify registration refinement. The estimated results are presented in Table 4.

Table 2: Evaluation results of first polymer sample. Averaged euclidean distance $\bar{\delta}$ in pixel units, between *interest points* before (b) and after (a) registration was estimated. Numerical indices refer to the corresponding point.

HS	$\bar{\delta}_{1b}$	$\bar{\delta}_{1a}$	$\bar{\delta}_{2b}$	$\bar{\delta}_{2a}$	$\bar{\delta}_{3b}$	$\bar{\delta}_{3a}$	$\bar{\delta}_b$	$\bar{\delta}_a$
IRMS _A	13.3	4.4	19.3	11.2	15.6	10.6	16.0	8.7
RMS _A	11.4	6.1	11.8	4.8	8.2	1.0	10.5	4.0
IRMS _M	12.3	6.6	18.3	7.9	15.0	8.5	15.2	7.7
RMS _M	11.9	6.2	12.0	1.5	8.0	0.7	10.6	2.8

Here, the numerical indices of the HSI corresponds to the considered polymer sample. The evaluation results show that the introduced methodology leads to clearly detectable refinements in registration accuracy. This improvement could be demonstrated for HSI of both modalities.

6. DISCUSSION

Based on a visual assessment of the estimated global gradient images presented in Fig. 3 reveals that the proposed methodology reliably extract prominent gradient information distributed in the spectral domain of the considered HSI. Solving the optimization problems defined in equation 5 and 9 leads to highly correlated images which can be considered as promising for intensity-based registration. These observations are support by the numeric results presented in Tables 2-4, which show a clear improvement in registration accuracy and correlate with the visual impression of the registration refinement achieved, as exemplary shown in Fig. 4. This contribution has demonstrated that the introduced approach enables a refinement in registration for already fine registered HSI, as well as for those providing major misregistration to the anchor image.

Table 3: Evaluation results of second polymer sample. Averaged euclidean distance $\bar{\delta}$ in pixel units, between *interest points* before (b) and after (a) registration was estimated. Numerical indices refer to the corresponding point.

HS	$\bar{\delta}_{1b}$	$\bar{\delta}_{1a}$	$\bar{\delta}_{2b}$	$\bar{\delta}_{2a}$	$\bar{\delta}_{3b}$	$\bar{\delta}_{3a}$	$\bar{\delta}_b$	$\bar{\delta}_a$
IRMS _A	47.9	12.0	25.0	1.3	46.9	9.4	39	7.6
RMS _A	38.8	5.2	28.4	0.5	27.9	6.25	31.7	4.0
IRMS _M	45.6	13.4	23.8	1.3	49.3	11.0	39.6	8.5
RMS _M	37.2	7.4	25.7	0.7	29.5	4.6	30.8	4.2

Nevertheless, it is obvious that a minimum degree of local correlation between the images of the considered modalities must be given initially, for the introduced approach to be reliably applicable. As the concept of global gradient estimation leads to registration refinement for IRMS and RMS data, it was found to be potentially independent concerning different spatial resolutions of the image data. With respect to the estimates of weighting vectors α and β , it was observed that the major gradient information for the reconstruction of ∇X and ∇Y were extracted from the highest and lowest level of the image decomposition, while the intermediate levels only provide minor or negligible contribution. This effect was observed for both spectroscopic modalities. Thus, the proposed methodology combines highly resolved details of the original image with the general gradient structure given by representations of lower resolution. Based on the visual assessment and the numeric results that were achieved within the context of this contribution, it can be concluded that the introduced concept of global gradient estimation leads to gradient images that are appropriate for refining the registration accuracy of HSI. This approach can thus be considered as a promising alternative to established state-of-the-art methodologies.

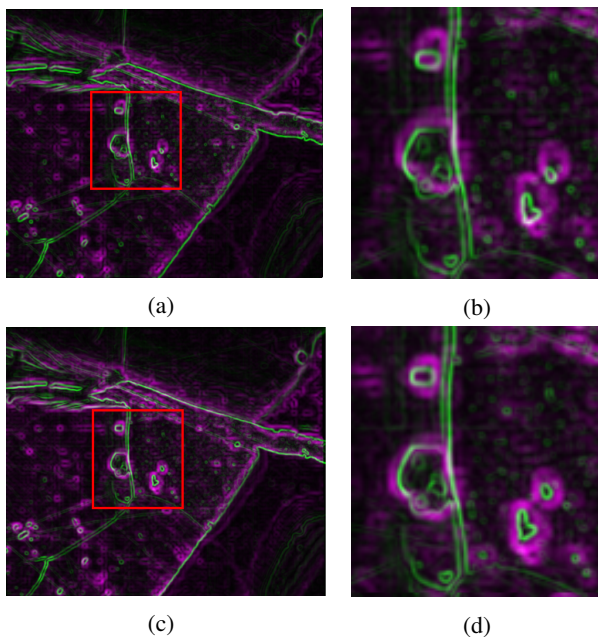


Fig. 4: Comparison of the initial registration accuracy between HSI and anchor image (a)-(b) and the registration refinement achieved by applying intensity-based registration to HSI data (c)-(d). Visualization before registration (a) and up-scaled region of interest. Visualization after registration refinement (c) and up-scaled region of interest (d). An improvement in registration accuracy is observable.

Table 4: Evaluation results of first and second polymer sample. Averaged euclidean distance $\bar{\delta}$ in pixel units, between *interest points* before (b) and after (a) registration was estimated. Numerical indices of $\bar{\delta}$ refer to the corresponding point. Numerical indices of HSI refer to the considered sample.

HS	$\bar{\delta}_{1a}$	$\bar{\delta}_{1b}$	$\bar{\delta}_{2a}$	$\bar{\delta}_{2b}$	$\bar{\delta}_{3a}$	$\bar{\delta}_{3b}$	$\bar{\delta}_a$	$\bar{\delta}_b$
HSI _{1A}	13.3	7.0	17.7	10.0	12.3	0.5	14.4	5.8
HSI _{1M}	14.9	11.4	20.6	10.9	12.2	6.5	15.9	9.6
HSI _{2A}	6.3	2.9	3.9	2.9	11.5	7.2	7.2	4.4
HSI _{2M}	6.2	0.5	5.1	3.4	9.3	5.6	6.87	3.18

7. CONCLUSION

In this contribution, the concept of global gradient estimation has been introduced as a new methodological approach of computing gradient images from hyperspectral image data for the purpose of registration refinement. It uses gradient information of an anchor image to estimate global gradient information that is distributed over the spectral domain of the hyperspectral image. The methodology has been investigated in the context of a multimodal imaging approach in vibrational microspectroscopy. It could be demonstrated that the proposed concept is leading to clearly observable improvements in the registration accuracy of the considered image data and outperforms comparable methods in terms of applicability. Using the proposed methodology, gradient images that are appropriated for intensity-based registration could be estimated for different initial degrees of misregistration and for the different spatial resolutions of the imaging modalities. It can be concluded that the implemented approach reliably extract gradient information distributed along the spectral domain of the hyperspectral image, leading to gradient images that are promising for refinements in intensity-based image registration.

8. REFERENCES

- [1] D. G. Lowe, "Distinctive image features from scale-invariant keypoints," *International Journal of Computer Vision*, vol. 60, 2004.
- [2] H. Bay, T. Tuytelaars, and L. Van Gool, "Surf: Speeded up robust features," in *Computer Vision – ECCV 2006*, 2006.
- [3] P. F. Alcantarilla, A. Bartoli, and A.J. Davison, "Kaze features," in *Computer Vision – ECCV 2012*, 2012.
- [4] Z. Yi, C. Zhiguo, and X. Yang, "Multi-spectral remote image registration based on sift," *Electronics Letters*, vol. 442, 2008.

- [5] A. Ordonez, F. Arguello, and DB. Heras, "Alignment of hyperspectral images using kaze features," *Remote Sensing*, vol. 10, 2018.
- [6] A. Ordonez, D. B. Heras, and F. Arguello, "Surf-based registration for hyperspectral images," in *IGARSS 2019 IEEE International Geoscience and Remote Sensing Symposium*, 2019.
- [7] J. T. Kwak, S. M. Hewitt, S. Sinha, and R. Bhargava, "Multimodal microscopy for automated histologic analysis of prostate cancer," *BMC Cancer*, vol. 11, 2011.
- [8] C. Yang, D. Niedieker, and F. Groerschkamp et al., "Fully automated registration of vibrational spectroscopic images in histologically stained tissue sections," *BMC Bioinformatics*, vol. 16, 2015.
- [9] A. A. Gowen and R. M. Dorrepaal, "Multivariate chemical image fusion of vibrational spectroscopic imaging modalities," *Molecules*, vol. 21, 2016.
- [10] F. Allouche, M. Hanafi, and F. Jamme et al., "Coupling hyperspectral image data having different spatial resolutions using multiple co-inertia analysis," *Chemometrics and Intelligent Laboratory Systems*, vol. 117, 2012.
- [11] F. Penaranda, V. Naranjo, and R. Verdu-Monedero et al., "Multimodal registration of optical microscopic and infrared spectroscopic images from different tissue sections: An application to colon cancer," *Digital Signal Processing*, vol. 68, 2017.
- [12] S. Trukhan, V. Tafintsev, and K. Tondel et al., "Grayscale representation of infrared microscopy images by extended multiplicative signal correction for registration with histological images," *Journal of Biophotonics*, vol. 13, no. 8, 2020.
- [13] H. Martens and E. Stark, "Extended multiplicative signal correction and spectral interference subtraction: New preprocessing methods for near infrared spectroscopy," *Journal of Pharmaceutical and Biomedical Analysis*, vol. 9, no. 8, 1991.
- [14] C. L. Lawson and R. J. Hanson, *Solving least square problems*, Prentice Hall, 1974.